

NRC Publications Archive Archives des publications du CNRC

The vertical pressure distribution on structures subjected to rubble-forming ice

Timco, Garry

This publication could be one of several versions: author's original, accepted manuscript or the publisher's version. /
La version de cette publication peut être l'une des suivantes : la version prépublication de l'auteur, la version acceptée du manuscrit ou la version de l'éditeur.

Publisher's version / Version de l'éditeur:

Proceedings of the 11th International Conference on Port and Ocean Engineering under Arctic Conditions, POAC '91, 1, pp. 185-197, 1991

NRC Publications Archive Record / Notice des Archives des publications du CNRC :

<https://nrc-publications.canada.ca/eng/view/object/?id=d68fea2e-5d04-4683-b5c3-80cdb1411970>

<https://publications-cnrc.canada.ca/fra/voir/objet/?id=d68fea2e-5d04-4683-b5c3-80cdb1411970>

Access and use of this website and the material on it are subject to the Terms and Conditions set forth at

<https://nrc-publications.canada.ca/eng/copyright>

READ THESE TERMS AND CONDITIONS CAREFULLY BEFORE USING THIS WEBSITE.

L'accès à ce site Web et l'utilisation de son contenu sont assujettis aux conditions présentées dans le site

<https://publications-cnrc.canada.ca/fra/droits>

LISEZ CES CONDITIONS ATTENTIVEMENT AVANT D'UTILISER CE SITE WEB.

Questions? Contact the NRC Publications Archive team at

PublicationsArchive-ArchivesPublications@nrc-cnrc.gc.ca. If you wish to email the authors directly, please see the first page of the publication for their contact information.

Vous avez des questions? Nous pouvons vous aider. Pour communiquer directement avec un auteur, consultez la première page de la revue dans laquelle son article a été publié afin de trouver ses coordonnées. Si vous n'arrivez pas à les repérer, communiquez avec nous à PublicationsArchive-ArchivesPublications@nrc-cnrc.gc.ca.

GARRY W. TIMCO
National Research Council
Ottawa, Ont. K1A 0R6
Canada

THE VERTICAL PRESSURE DISTRIBUTION ON STRUCTURES SUBJECTED TO RUBBLE-FORMING ICE

ABSTRACT - A laboratory test program has been performed on ice loading through pressured broken ice. The results have applications to both structures and ships in Arctic regions. The work was performed by measuring the loads on a segmented planar structure for various loading conditions. The variables included ice strength, ice thickness, ice density, ice/structure friction and angle of inclination of the structure. Vertical distributions of loads, point of resultant load application and overturning moments have been examined. A comparison of extrapolated peak pressures show excellent agreement with full-scale measurements on the Gulf Canada's arctic structure Molikpaq.

INTRODUCTION

In the Arctic, broken ice plays an important role in several situations. For example, it is known that broken ice can accumulate as floating or grounded rubble beside offshore drilling structures. Also, broken ice can be generated along the side of a ship. If this ice is pressured by an advancing ice sheet driven by environmental forces, the broken ice will transmit this load to the structure or ship. For a structure, this has important implications in terms of the load distribution on its face. For a ship, this could lead to a high overturning moment, large ice pressure and ice overtopping. To date, very little is known about this problem.

The National Research Council of Canada and the Canadian Coast Guard have collaborated to conduct research in this area. There are several research tasks in this area, and the work reported here forms only one part of the full research program. The present paper centres on a description of a model test series to investigate the behaviour of broken ice pressured against a rigid structure. To perform these tests, an idealized two-dimensional model was designed and constructed. The model was designed to represent a plane-surface that could be rotated through an angular range of $\pm 30^\circ$ from the vertical. In addition, since the loads and load distribution were of interest, the plane was segmented in six sections so that a vertical pressure distribution on the model could be obtained.

EXPERIMENTAL

The tests were performed in the ice tank at the Institute of Mechanical Engineering in Ottawa. This tank, which is 21 m long, 7 m wide and 1 m deep, is spanned by a carriage. The model structure was mounted to this carriage, and the ice loads were measured as the carriage was driven along the tank.

The general concept is depicted in Figure 1, which shows a side view of the carriage in the ice tank and the various components of the design. A large bracket containing a circular track was mounted to the front face of the carriage. This track supported the basic frame for the model and allowed it to be rotated to angles of $\pm 30^\circ$ from the vertical. The chosen sign convention is a positive value for the case when the model is inclined back from the advancing ice sheet (see Figure 1). A feature of the apparatus was that the centre of rotation was at the waterline and thus changes in inclination angle did not change the nominal level of ice action. The front face of the structure was divided into 6 horizontal segments, 2 above the waterline and 4 below. Each segment, of dimension 15 cm high by 95 cm wide, was supported by a 5-component dynamometer which allowed the normal and tangential load on each segment to be measured. With this design and appropriate instrumentation, the total loads and moments on the plane could be measured, as well as the vertical distribution of normal and tangential loads. In addition, by re-coating the segments, the ice/structure friction coefficient could be set at any desired value. Two different friction coatings were used on the model, with measured static and dynamic friction coefficients of 0.06 and 0.04 for the low friction coating, and 0.83 and 0.40 for the high friction coating.

The tests were arranged such that ice behaviour was essentially two-dimensional; i.e., in the direction of motion of the carriage and vertically perpendicular to that direction (x and z directions - see Figure 1). This was accomplished by positioning vertical side walls adjacent to either side of the structure in order to restrict horizontal transverse motions of the ice. Since it was desirable to observe the ice during the test, two plexiglass sides were used for this purpose (see Figure 2), forming a "chute" arrangement. Note that the two plexiglass walls were mounted independent of the test structure. Slots were cut in the ice in front of each plexiglass side, leaving a tongue of ice slightly narrower than the "chute" to come in contact with the structure. With this arrangement and a video camera photographing the tests, it was possible to identify the various processes occurring throughout the interaction events, and measure the size of the rubble accumulation. For a few tests, an underwater video camera was used to show the detailed behaviour of the keel of the ice rubble.

For the test, the model was mounted on the front of the carriage, and it was slowly driven along the full length of the tank at a rate of $2 \text{ cm}\cdot\text{s}^{-1}$. At this rate, it took approximately 510 s (8.5 minutes) to travel a length of 10.2 m. As the test progressed, a large pile of broken ice would accumulate in front of the structure. Thus, for the latter part of the time series, the structure was loaded through pressured broken ice. During the test, the output from all of the instrumentation was measured at a rate of 20 Hz with a 10 Hz anti-aliasing filter. The data were stored on disk and magnetic tape for subsequent data analysis.

For the tests, EG/AD model ice was used (Timco, 1986). For a number of tests, use was made of a new technique to produce correct density (CD) ice (Spencer and Timco, 1990). This technique involves the use of a submarine carriage which travels under the growing ice sheet, releasing small air bubbles. These air bubbles are

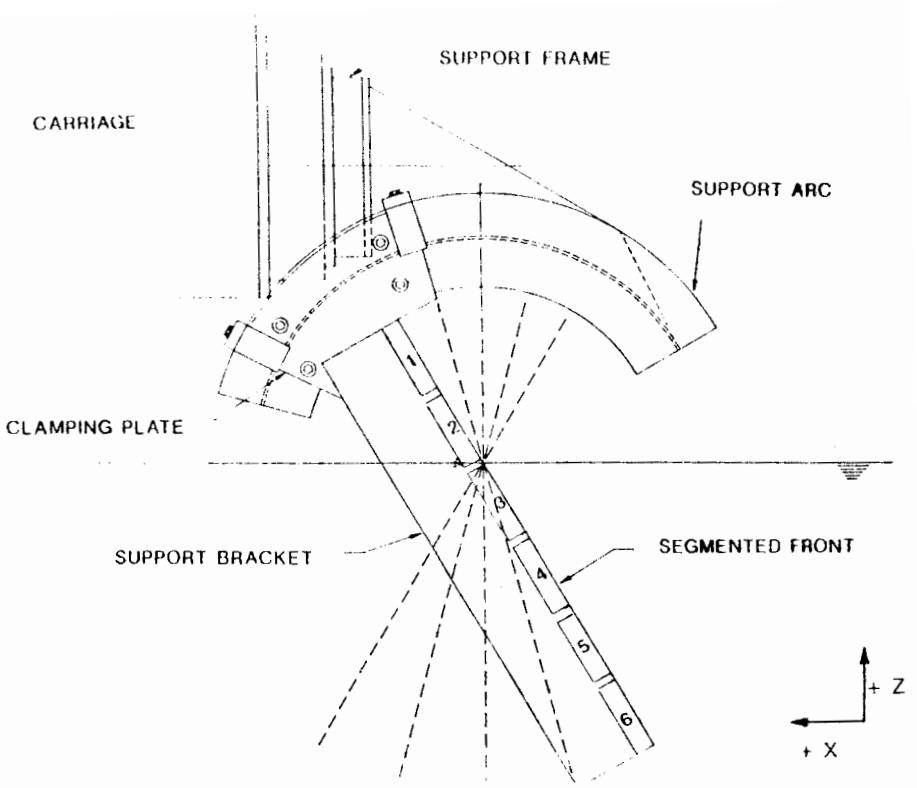


Figure 1: Schematic showing a side view of the experimental arrangement.

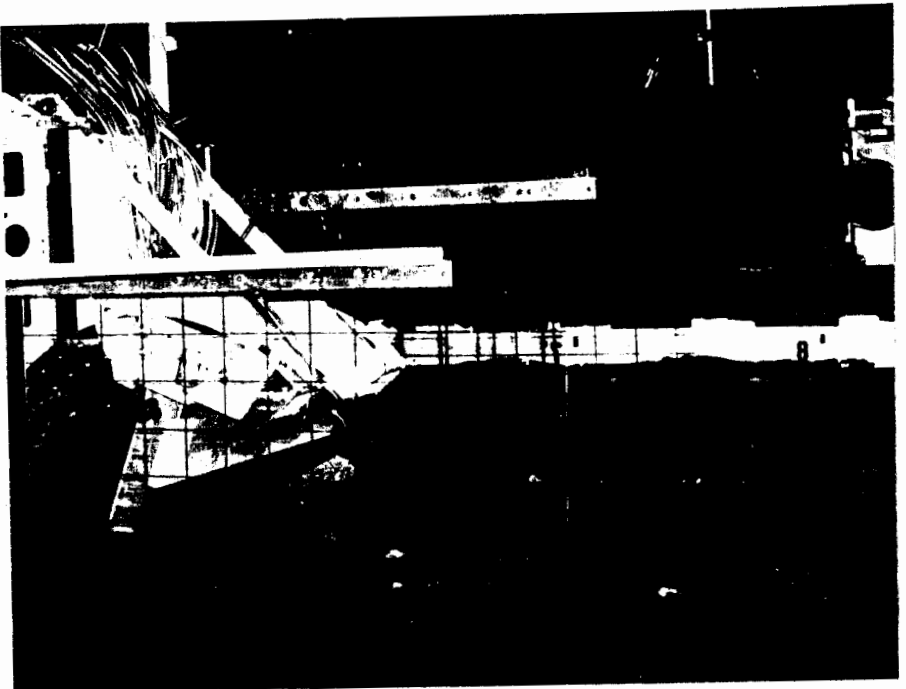


Figure 2: Photograph of the test assembly.

trapped in the growing ice sheet and result in a lower density ice, giving ice densities of 0.87-0.89 gm-cm³. For one test, the density was lowered to 0.79 gm-cm³.

RESULTS

At the start of each test, no ice was touching the model. As the carriage was driven along the length of the tank, the ice would contact the structure, and fail, usually by buckling. With further advance of the structure, more ice would contact it and a natural rubble pile would start to form in front. By the end of the test, a pile of broken ice would be in front of the structure. The size of the pile was a function of the angle of inclination of the structure. For tests where the structure was inclined towards the advancing ice sheet with a negative inclination angle greater than 15°, as much as one-third of the ice would slide down the face of the model and exit from underneath it. However, for other loading configurations, all of the broken ice would stay in front of the structure, and much larger rubble piles would form.

In total, 22 ice sheets were used, giving 22 test files named TN_x where x ranges from 1 to 22 (Timco, 1991). The parameters that were varied include the angle of the model from the vertical position (α), friction (μ) of the structure, and ice flexural strength (σ_F), thickness (h_i) and density (ρ). The values for each of the 22 tests are listed in Table 1. The tests produced a considerable amount of experimental data (see Timco (1991) for a full compilation). In summary, for each of the 22 tests, the following information is available:

1. Time series of the normal, tangential and resultant loads for each of the six segments, as well as the total loads on the model.
2. The point of load application relative to the water line (i.e., the moment arm) and the overturning moment on the structure relative to the water line.
3. A schematic illustration of the geometric evolution of the ice rubble in front of the structure as a function of time. Also, an estimate of the residual volume of broken ice is presented as a function of time during the whole loading event.
4. A depth histogram for each test based on the measured maximum, mean and minimum value for each test.
5. Probability density and cumulative distribution of the loads on each segment. These are also presented for normal, tangential and resultant loads.

In addition, 13 individual loading events were isolated and the behaviour of the loads during the course of the loading event were examined.

GENERAL DISCUSSION

In observing the tests, it was evident the ice could fail in many different ways. On several occasions, the ice would fail in a bending or flexural-type failure. The

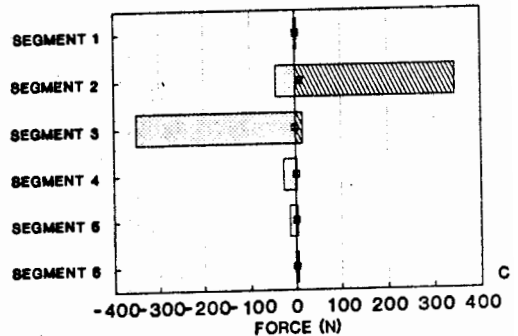
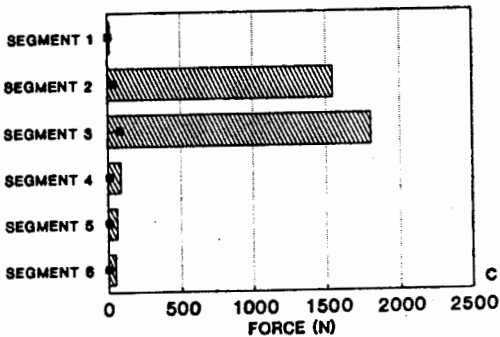
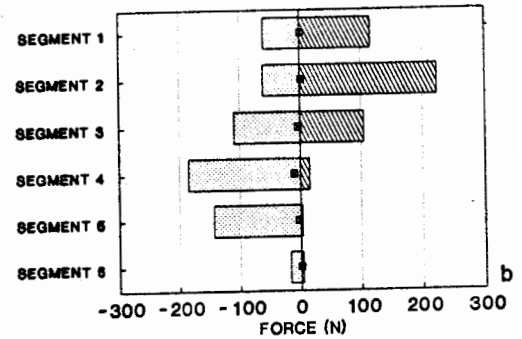
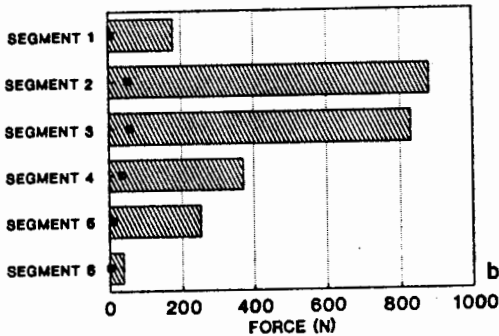
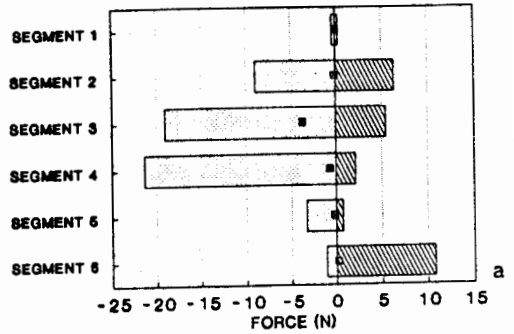
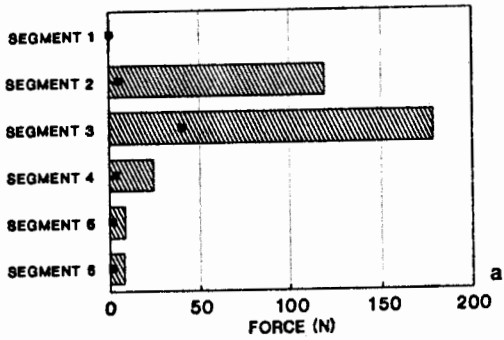
advancing ice sheet would usually ride up over the ice rubble and fail as it pushed against the sail of the rubble close to the structure. Depending on the angle of the model, the bending failures could be either up or down. Large-scale buckling was a frequent mode, especially in the early part of the test when there was little rubble in front of the structure. Ice crushing was also observed to occur, especially in small local crushing events. Large-scale ice splitting occurred on a few occasions. The details of the ice/structure interaction were a function of the angle of the structure. Figure 3 shows the measured values of the average and extreme normal and tangential loads on each segment of the structure for three different angles of inclination; ($\alpha = -23$ for Figure 3a, $\alpha = 24^\circ$ for Figure 3b, and $\alpha = 0^\circ$ for Figure 3c).

TABLE 1. Details of the set-up for each test.

FILE NAME	FLEXURAL STRENGTH	ICE DENSITY	ICE THICKNESS	ANGLE OF PLANE	FRICTION	BUBBLED ICE
	(kPa)	(g/cm ³)	(cm)	(degrees)		
TN_001	106	0.93	3.1	-23	LOW	NO
TN_002	44	0.93	3.6	-23	LOW	NO
TN_003	83	0.93	2.8	-23	LOW	NO
TN_004	70	0.93	3.5	-15	LOW	NO
TN_005	86	0.93	3.3	-5	LOW	NO
TN_006	64	0.93	3.2	0	LOW	NO
TN_007	101	0.93	3.5	8	LOW	NO
TN_008	85	0.93	3.5	15	LOW	NO
TN_009	62	0.93	3.6	24	LOW	NO
TN_010	60	0.87	3.1	24	LOW	YES
TN_011	94	0.89	3.3	13	LOW	YES
TN_012	58	0.88	3.2	0	LOW	YES
TN_013	53	0.85	3.2	-10	LOW	YES
TN_014	39	0.89	3.4	-30	HIGH	YES
TN_015	35	0.89	3.4	-12	HIGH	YES
TN_016	64	0.88	3.3	0	HIGH	YES
TN_017	50	0.90	3.4	24	HIGH	YES
TN_018	61	0.85	3.0	7	HIGH	YES
TN_019	24	0.93	2.3	7	HIGH	YES
TN_020	15	0.93	3.6	7	HIGH	YES
TN_021	24	0.93	2.6	7	HIGH	YES
TN_022	21	0.79	3.8	7	HIGH	YES

NORMAL

TANGENTIAL



■ F_n MEAN ▨ F_n MAX

■ F_t MEAN ▨ F_t MAX □ F_t MIN

Figure 3: Measured average and extreme values of the normal and tangential loads on each segment for a) negative angle of inclination ($\alpha = -23^\circ$, TN_002); b) positive angle of inclination ($\alpha = 24^\circ$, TN_017); c) vertical structure ($\alpha = 0^\circ$, TN_012).

In Figure 3a, where the structure was inclined towards the advancing ice sheet with a negative slope of -23° (Test TN_002), the ice tended to load the structure directly at the waterline. Thus, there were high normal loads on the structure in the waterline region (segments #2 and #3). Although there could be some local crushing, the ice usually failed in a bending or buckling mode. The newly broken ice pieces would rotate and slide down the face of the model. There was very little pile-up of ice in front of the structure. Also, as shown in Figure 3a, the ice never touched the upper segment (#1) of the model.

In the opposite inclination, where the model was inclined away from the advancing ice sheet (positive slope), different behaviour occurred. Figure 3b shows the loads on the segments for test TN_017 with a positive angle of inclination of 24° . The highest ice loads occurred in the waterline region of the structure. In this case, however, the broken ice tended to ride up the model creating both tangential and normal loads on the upper segments of the structure (Figure 3b). Broken ice pieces would form a small sail in the region in front of the structure. Then, subsequent loading events occurred by loading the structure through a layer of ice rubble. Thus, the advancing ice sheet loaded the structure through only a few pieces of ice rubble, and the ice sheet was buoyantly supported from below by a large mass of broken ice. In this case, there was much more ice crushing, and, occasionally, large scale ice splitting. In the cases where a relatively large sail developed through ice ride-up, the ice would accumulate on top of the rubble until a critical level was reached. At that time, a large-scale bending failure of the ice would occur, and the sail of the rubble would slide down the face of the structure. This would lead to negative tangential loads on a number of segments simultaneously.

When the model was vertical, or near vertical, the ice behaviour was quite similar to the case with a positive angle of inclination. Figure 3c shows the average and extreme loads on each segment for a test with a vertical structure face (test TN_012). Contrary to the other cases, however, almost all of the ice loads are always at the waterline region, with very little loading elsewhere. Ride-up and pile-up does occur, but not to the extent seen for tests with high positive angles of inclination. It was possible to isolate individual loading events and monitor the details of the loads and load application points throughout the whole event. This was done for a number of individual events. The analysis clearly showed the complexity of the whole process. One example is shown in Figures 4 to Figure 6. Figure 4 shows the total loads on the structure for one loading event in test TN_018 with the model at an angle of 7° , high friction coefficient surface, ice thickness of 3.0 cm, ice flexural strength of 61 kPa, and an ice density of 0.85 g-cm^{-3} . The sign convention chosen for the tests is positive in the directions shown on Figure 1. This loading event lasted 25 s, and occurred at a time of 340 s from the start of the test. Individual plots of the loads on each segment are shown in Figure 5. Note here the high normal forces on segments 2 and 3. Also, note that the tangential load is large and positive on segment 2 and is large and negative on segment 3. (Recall that the waterline is at the junction between segments 2 and 3). These plots were analyzed, such that every 5 seconds, the measured value on the segments were noted. These values were then plotted in a histogram form to give a time-sequence of the ice loading event. Figure

6 shows the loading behaviour on the structure for both the normal and tangential loads. Note that the load is primarily centred at the waterline, and that there is considerable variation of load in the vertical direction of the structure. The sequence described above was unique to that one particular loading event. Each such event showed differences in the details of the behaviour.

The underwater camera provided useful information on the behaviour of the rubble below the water line. In many tests, the ice rubble would exhibit behaviour whereby the whole rubble pile would "roll" in a circular fashion in the direction of the advancing ice sheet. Because of this, a considerable amount of the broken ice would be turned upside down from its original orientation. If there were a wide range of ice piece sizes in the rubble, the rolling events would reorganize the rubble and give the rubble a more random orientation of ice pieces.

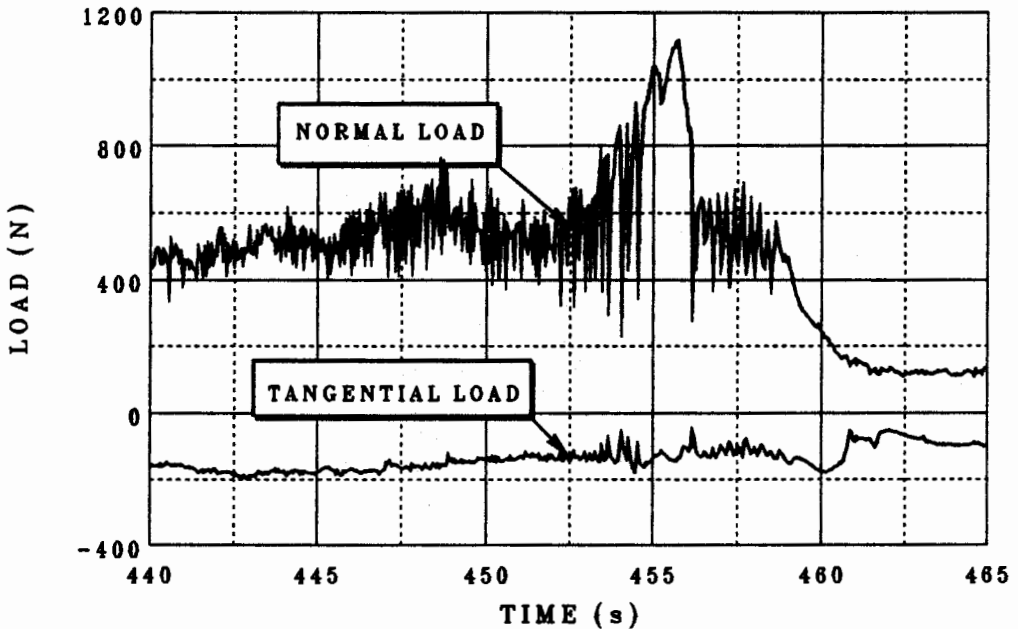
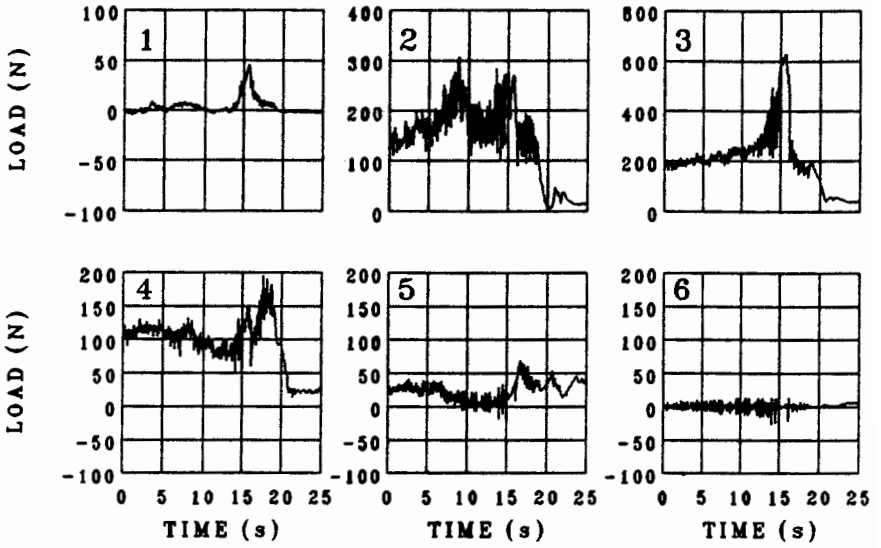


Figure 4: Total normal and tangential loads on the structure during a loading event for test TN_018.

NORMAL LOAD



TANGENTIAL LOAD

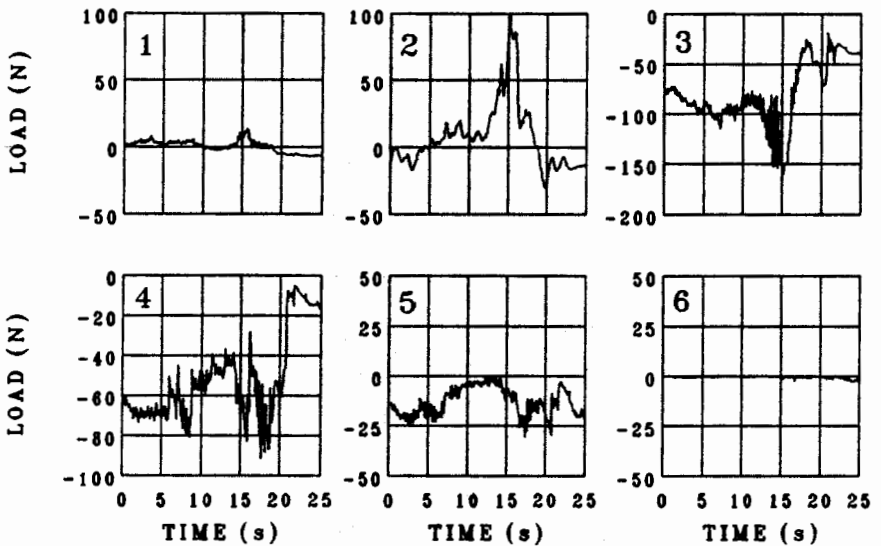


Figure 5: Load-time traces for each of the six segments during the loading event shown in Figure 4. The top six traces show the normal load, and the bottom six traces show the tangential loads. (Test TN_018);

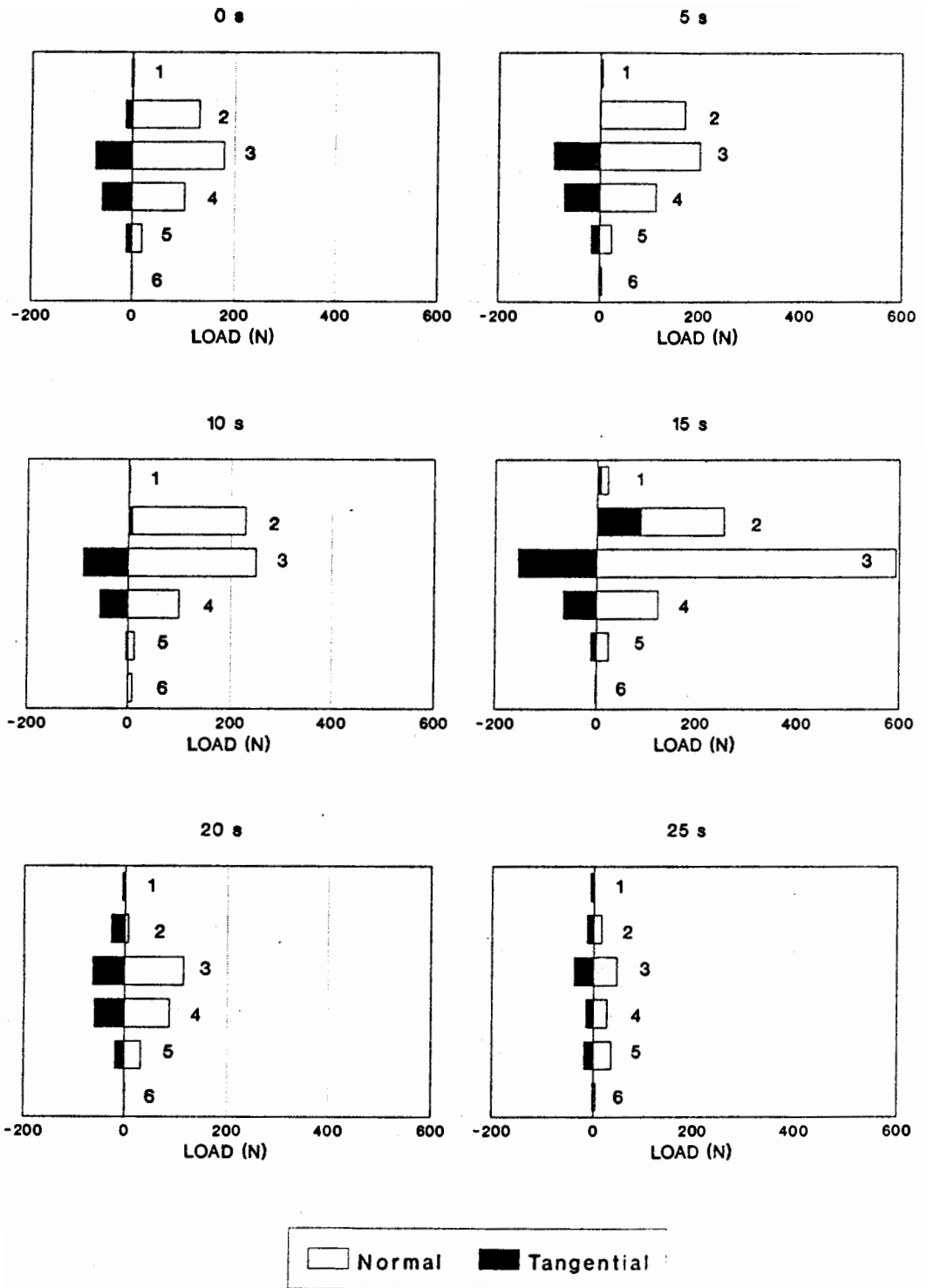


Figure 6: Time sequence of the normal and tangential loads on the structure versus depth for the loading event shown in Figures 4 and 5. (Test TN_018).

COMPARISON TO THE MOLIKPAQ 1984/85 DATA

As part of the entire investigation into this problem, an analysis was made of the loading events on the Gulf Arctic structure "Molikpaq" and, in particular, of the vertical and horizontal load distribution on it during loading events. For the year 1984/85, the results of the rubble-building events are in the public domain (Neth, 1989, 1991). In this year, Neth identified three rubble-building events. The details of the events are too voluminous to present here. A qualitative description of the ice loading events in the full-scale situation were in very good agreement with the test results reported here. Several of the failure modes observed in the field situation were observed in the model tests including bending failures, ice ride up, ice crushing and large-scale bending due to ice accumulation in the sail of the rubble ice.

Although there are uncertainties, it is possible to make a quantitative comparison between the pressure data from the Molikpaq and the present test results. From Neth's analysis, the three events had the characteristics given in Table 2. The values represent the peak value of the ice pressure on one of the long faces of the structure. For these three events, the ice thickness was 0.6 to 0.7 m. The first event took place in mid-winter when the ice was cold and strong; the latter two events took place in spring when the ice was warmer and weaker. To compare this to the present tests, it is necessary to make a few statements about the type of comparison that can be made. In the present test program, there was no intention to try to scale identically the results presented by Neth on the Molikpaq. The present tests were concerned with a two-dimensional situation. For this, the individual sensing panels are quite long relative to the thickness of the ice, giving a high aspect ratio. For the field condition, the panels are small relative to the width and height of the structure, and they are comparable in size to the thickness of the ice. More importantly, they only cover approximately one-tenth of the face of the structure. Thus, in the model test, the full global load was measured, whereas in the full-scale situation, the load was measured over a small part of the structure, and the load was extrapolated to represent the load on the full face of the structure.

TABLE 2. Characteristic of full-scale results.

EVENT NUMBER	ICE THICKNESS	PEAK PRESSURE	TIME OF EVENT
	m	MPa	
33R	0.7	1.2, 0.9	Feb 15/16
44R	0.6	0.5	April 10
45R	0.6	0.8	April 11

To compare to the first Molikpaq event, which had a strong ice sheet, four tests have similar conditions (TN_006, TN_012, TN_016, TN_018). For the loading events in April, the ice would be relatively weak. Three of the tests from the present series

can be used in this comparison (TN_020, TN_021, TN_022). Note that these tests all have angles of inclination ranging from 0° to 7° from the vertical, close to that of the Molikpaq (7°).

To scale these results, it is necessary to choose a scale factor. A simple approach would be to choose a scale factor based on the ice thickness (h_i). Thus, the scale factor (λ) would be

$$\lambda = h_i(\text{full scale}) / h_i(\text{model scale}). \quad (1)$$

For example, for test TN_018 (shown in Figures 4 to 6), the model ice had a thickness of 3.0 cm. Since the full-scale ice thickness was 0.7 m (70 cm), this would give a scale factor of (70 cm / 3.0 cm) 23.3. Scaling of the model ice strength by this scale factor would give a full-scale flexural strength of (61 * 23.3) = 1.4 MPa and a full-scale compressive strength of 3.0 MPa. These strength values are representative of a strong sheet of ice, so the strength comparison is reasonable. For this test in the ice tank, the peak load on the whole structure was 1.1 kN. From this value, the peak global pressure can be determined from

$$P = F_{N_tot} / (w * h_i) \quad (2)$$

where F_{N_tot} is the peak force on the structure, and w is the width of the structure (= 0.95 m). This is the definition used by Neth in calculating the global pressure on the face of the Molikpaq. For test TN_018, the peak pressure was 38.6 kPa. If this measured pressure is scaled according to the Froude scaling laws, directly with λ , the predicted peak pressures in the full-scale situation would be 0.9 MPa. This is in excellent agreement with the full-scale peak pressures of 0.9 and 1.2 MPa. Similarly, as given in Table 3, the other six tests with inclination angles of 0° and 7° were used to predict the full-scale pressure values.

TABLE 3. Comparison of model and full-scale results.

MODEL TESTS					FULL SCALE				
TEST NUMBER	h_i	σ_F	PEAK FORCE	PEAK PRESSURE	SCALE FACTOR	σ_F	PREDICTED	EVENT #	MEASURED
							PEAK PRESSURE		PEAK PRESSURE
	cm	kPa	kN	kPa		MPa	MPa		MPa
TN_006	3.2	64	1.3	42.8	21.9	1.4	0.94	33R	0.9, 1.2
TN_012	3.2	58	2.1	69.1	21.9	1.3	1.51	33R	0.9, 1.2
TN_016	3.3	64	1.6	51.0	21.2	1.4	1.08	33R	0.9, 1.2
TN_018	3.0	61	1.1	38.6	23.3	1.4	0.90	33R	0.9, 1.2
TN_020	3.6	15	0.83	24.3	16.7	0.25	0.40	44R,45R	0.5, 0.8
TN_021	2.6	24	0.57	23.1	23.1	0.55	0.53	44R,45R	0.5, 0.8
TN_022	3.8	21	1.3	36.0	15.8	0.33	0.57	44R,45R	0.5, 0.8

The measured and predicted values in Table 3 shows quite remarkable agreement. The excellent agreement in the present tests, both in terms of the qualitative description of the rubble-building events and the predicted global pressures on the structure, gives confidence in the measured results.

SUMMARY

A test program has been performed to measure the vertical distribution of loads on a structure. Several parameters were varied during the course of the tests. The results of the tests are quite voluminous, and they are reported in full in Timco (1991). In general, the vertical distribution of loads on a structure is complex. However, even with a floating rubble pile in front of the structure, the majority of load is transmitted to the structure at the waterline.

ACKNOWLEDGEMENTS

This work formed part of a collaborative effort between the National Research Council and the Canadian Coast Guard. The author would like to thank Mr. Victor Santos-Pedro and Mr. John McCallum of the CCG for their interest in this project. The author thanks Ed Funke for his work relating to the design of the test apparatus. Ed Arambarri, Janet Williams and Ruth Abraham, three engineering students from Memorial University, were instrumental in this test program. Finally, the author thanks Jeff Farnand for his usual high standard of technical assistance during the course of this test program.

REFERENCES

- Neth, V. 1989. Rubble Formation Along the Molikpaq at Tarsiut P-45 during 1984/85. Report prepared for the National Research Council, Ottawa, Canada.
- Neth, V. 1991. Ice Rubble Formation along the Molikpaq. *Proc. POAC'91*, St. John's, Nfld., Canada (this volume).
- Spencer, D.S. and Timco, G.W. 1990. CD Model Ice: A Process to Produce Correct Density Model Ice. *Proc. IAHR Ice Symposium*, Espoo, Finland, Vol. 2, pp. 745-755.
- Timco, G.W., 1986. EG/AD/S: A New Type of Model Ice for Refrigerated Towing Tanks. *Cold Reg. Sci. and Tech.*, Vol. 12, pp. 175-195.
- Timco, G.W., 1991. Model Tests of Pressured Broken Ice on a Segmented Inclined Plane. *National Research Council Report TR-LT-021*, Ottawa, Ont., Canada.